Theoretical Approaches to Direct Exchange Couplings between Divalent Chromium Ions in Naked Dimers, Tetramers, and Clusters

Masamichi Nishino, Syusuke Yamanaka, Yasunori Yoshioka, and Kizashi Yamaguchi*

Department of Chemistry, Graduate School of Science, Osaka University, Toyonaka, Osaka 560, Japan

Received: July 16, 1996; In Final Form: September 30, 1996[⊗]

Direct exchange interactions between divalent chromium ions in naked dimers, tetramers, and clusters were investigated theoretically. The orbital energy gaps, occupation numbers, and bond orders for the naked Cr(II)−Cr(II) dimer (**1**) were calculated by ab initio UHF MO and density functional (DFT) methods. All these calculations indicated that the orbital energy gaps are very small for **1**, and therefore the occupation numbers of the bonding σ, π, and δ molecular orbitals and formal quadruple bond orders were largely reduced because of strong electron correlation effects. The UHF and DFT MO calculations were also performed for the linear naked Cr(II) tetramer to elucidate possible electronic structures of the d−d conjugated systems. The energy differences among singlet, triplet, and quintet states for **1** were calculated from the total energies obtained by the CASCI and CASSCF methods based on the UHF and DFT natural orbitals (UNO). The reliability of the Heisenberg model Hamiltonian was elucidated from variations of these calculated effective exchange integrals with the interatomic distance. The calculated J_{ab} values are compared with the experimental results for several binuclear Cr(II) complexes with different interatomic distances. The Heisenberg spin Hamiltonian was used to discuss the spin alignments in large d−d conjugated Cr(II) clusters and a possibility of the macroscopic quantum spin tunneling in mesoscopic magnetic systems.

1. Introduction

Electronic structures of transition-metal dimers and clusters vary from the closed-shell nonmagnetic state, through intermediate states, to the non-closed-shell states with unpaired electrons. The closed-shell molecular orbital (MO) method has been extensively and successfully applied to elucidate the electronic properties of nonmagnetic metal clusters. The MO pictures for these species have been well accepted in relation to the so-called 18-electron rule. In past decades, the extended Hückel MO and spin-restricted density functional theories (DFT)[1] based on the scattered wave (SW) approximation were heavily utilized for the purpose.[2] On the other hand, it has been regarded that the MO treatments break down for non-closed-shell species such as magnetic clusters. Alternately, the VB-like models such as the Heisenberg model have been utilized to describe the direct exchange couplings between transition-metal ions and their superexchange couplings in relation to molecule-based magnetism.[3] Thus the nature of the metal−metal bonds in clusters is variable from the MO limit (strong covalent bond) to the VB limit (weak covalent bond), depending on several structural factors and component transition-metal ions.

Cotton et al.[1,4] have extensively investigated the quadruple metal (M)−metal (M) bonds for the M_2X_8 complexes (M = Cr, Mo, Re, etc.). The transition-metal ions MX_4 in these dimers are formally regarded as the d^4 configuration with the octahedral (O_h) ligand field. The quadruple M−M bonds have been described as the $\sigma^2\pi^4\delta^2$ orbital configuration on the basis of the spin-restricted MO theoretical picture. Cotton et al.,[1,4] however, performed magnetic measurements and solid state NMR spectroscopy of $Cr_2(O_2C\mathbf{R})_4L_2$ compounds (L = MeOH, etc.) that exhibited the weak temperature-dependent paramagnetism. They found that the direct exchange couplings between the Cr(II) ions are rather weak: the direct exchange integrals (J_{ab}) in the Heisenberg model are in the range −250 to −500 cm^{-1}.[5] These findings support the VB-like description of the weak Cr(II)−Cr(II) bonds: $(d\sigma)_a^1(d\sigma)_b^1(d\pi)_a^2(d\pi)_b^2(d\delta)_a^1(d\delta)_b^1$, where d*X* denotes the d atomic orbital (AO) on the atom *c* (*c* = a, b). Judging from these results, a systematic theoretical study from the MO to the VB region is desirable for full understanding of the multiple metal−metal bonds for the Cr(II) ion.[6]

Previously, we have examined the instability of the metal−metal bond and have shown the bifurcation of the closed-shell δ MO of **1** and the naked Mo(II)−Mo(II) dimer (**2**) into the dδ AOs, $(d\delta)_a$ and $(d\delta)_b$, on the basis of the DFT-like model calculations[7] and the ab initio unrestricted Hartree−Fock (UHF) and DFT calculations.[8] The antiferromagnetically coupled zero-valent manganese dimer $Mn(0)_2$ (**3**)[9a] and chromium dimer $Cr(0)_2$ (**4**)[9b] were also examined by the approximate spin-projected (AP) UHF Møller−Plesset perturbation (APUMP) method.[9] The calculated J_{ab} value for **3** was compatible with the experimental results.[10] The direct triple bond between Cr(III) ions in the superexchange-coupled systems was examined by APUMP,[9a] but it was found to be too weak for reasonable explanation of their antiferromagnetic exchange interactions. The superexchange interactions between the transition-metal ions through dianions, M−Y−M (**5**) (M = Cr^{3+}, Mn^{2+}, Fe^{3+}, etc.; Y = O^{2-}, S^{2-}), were examined by APUMP in relation to the ferro- or antiferromagnetism of the transition-metal oxides[9d] and sulfides.[9c] The results are wholly compatible with the experiments.[3,9]

As a continuation of previous work,[8,9] we examine here several theoretical approaches to the d−d conjugated systems. First, the unstable quadruple metal−metal bonds of **1** are thoroughly investigated by ab initio UHF and DFT methods, and complete active space (CAS) configuration interaction (CI) and CASSCF methods based on the UHF and DFT natural orbitals (UNO).[6] The occupation numbers of the occupied σ, π, and δ orbitals and formal quadruple bond orders are calculated by these methods. The energy differences among singlet, triplet, and quintet states for **1** are also calculated from the total energies obtained by the UNO CASCI and CASSCF methods. The reliability of the energy splittings predicted by the Heisenberg model Hamiltonian is examined from variations of the calculated effective exchange integrals and energy

[⊗] Abstract published in *Advance ACS Abstracts,* January 1, 1997.

S1089-5639(96)02091-9 CCC: $14.00

TABLE 1: Orbital Energy Gaps (eV) Calculated for the Naked Cr(II) Dimer (Cr_2^{4+}) by the High-Spin UHF, U-BLYP, and U-B2LYP Methods

	$\Delta\epsilon_{UHF}$			$\Delta\epsilon_{U\text{-}BLYP}$			$\Delta\epsilon_{U\text{-}B2LYP}$		
R/Å	$\sigma\sigma^*$	$\pi\pi^*$	$\delta\delta^*$	$\sigma\sigma^*$	$\pi\pi^*$	$\delta\delta^*$	$\sigma\sigma^*$	$\pi\pi^*$	$\delta\delta^*$
2.000	4.457	3.002	0.531	3.937	2.717	0.505	4.233	3.115	0.607
2.015	4.366	2.904	0.508	3.863	2.631	0.482	4.159	3.021	0.583
2.389	2.560	1.265	0.170	2.274	1.166	0.193	2.674	1.399	0.209
2.500	2.158	0.986	0.124	1.936	0.917	0.144	2.322	1.112	0.155
3.000	0.931	0.311	0.028	0.898	0.311	0.038	1.139	0.389	0.040
3.500	0.340	0.090	0.006	0.361	0.100	0.010	0.470	0.128	0.010

splittings with the interatomic distance. The calculated J_{ab} values for **1** are compared with the experimental results for several binuclear Cr(II) complexes with different interatomic distances.[5] This comparison may in turn provide significant information for a contribution of the through-ligand effective exchange interactions in the complexes. The linear naked Cr(II) tetramer (**6**) is also examined to elucidate the d−d conjugation effects from the UHF and DFT calculations. These calculations clarify the instability of the d−d bonds and spin populations for **6**. Finally, possible electronic states in magnetic metal clusters are briefly discussed in relation to the macroscopic quantum tunneling in mesoscopic transition-metal systems.[11]

2. MO-Theoretical Calculations of Binuclear Transition-Metal Systems

The MO-theoretical background[6] is explained here by using the direct exchange-coupled naked chromium(II) dimer (**1**). The ground state of the divalent chromium ion $Cr(d^4)$ is quintet. Therefore, **1** is regarded as the antiferromagnetically exchange-coupled d^4-d^4 system with a quadruple bond.[1] However, the strong electron correlation effect may reduce the formal bond order as in the cases of the direct exchange-coupled manganese dimer (**3**)[9a] and chromium dimer (**4**)[9b] and superexchange-coupled transition-metal complexes (**5**)[9c,d] examined previously. Here, the ab initio UHF MO calculations of **1** were carried out using the Tatewaki−Huzinaga basis set[12] [533(21)/53(21)/(41)+diffuse d(α=0.0912)], which was supplemented by the 4p AO with the same exponent as that for the 4s AO. The same triple-ζ (TZ) basis set was also utilized for the spin-unrestricted (U) DFT calculations by the use of the Becke−Lee−Yang−Parr (U-BLYP) functional[13,14] and Becke's mixing (U-B2LYP) methods. In the latter approach, the original mixing ratio between the UHF and DFT exchange terms ($c_0 = 0.332$ and $c_1 = 0.575$) by Becke[13b] was taken throughout this work. All the MO computations were carried out on the IBM RS 6000 computer using the GAUSSIAN 94 program package.[15]

2.1. UHF and DFT Calculations. We first examined the highest spin (HS) state of **1** based on the UHF and DFT methods since the SCF procedure is often divergent for the lowest spin (LS) singlet state.[6] The bonding and antibonding orbitals for the HS ($S = 4$) state of **1** are given by the spatial symmetry-adapted MOs,

$$\phi(X) = N[dX_a + dX_b], \quad \phi^*(X) = N'[dX_a - dX_b] \qquad (1)$$

where N (N') is the normalizing factor and dX denotes the d atomic orbital symmetry, i.e., σ, π_x, π_y, δ_{xy}, and $\delta_{x^2-y^2}$. The shapes of the σ, π, and δ MOs by HS UHF solutions are similar to those of the extended Hückel MO and DFT(SW) methods.[1] The orbital energy gaps are calculated to elucidate the strength of the d−d orbital interactions by

$$\Delta\epsilon_Y(X) = \epsilon^*(X) - \epsilon(X) \qquad (2)$$

where ϵ and ϵ^* denote, respectively, the orbital energies for the bonding and antibonding MOs by the HS UHF (=X) solution. Table 1 summarizes the energy gaps for σ, π, and δ MOs for **1** by UHF, together with U-BLYP and U-B2LYP. From Table 1, the energy gaps given by these methods are not so different, but they decrease in the order $\Delta\epsilon(X)_{U\text{-}B2LYP} \cong \Delta\epsilon(X)_{UHF} > \Delta\epsilon(X)_{U\text{-}BLYP}$. Judging from these small gaps, the bonding and antibonding orbitals are nearly degenerate in energy at a relatively large interatomic distance ($R > 2.3$ Å). As we reported previously,[6,7] the small energy gap indicates that the spin-restricted (closed-shell) Hartree−Fock (RHF) and spin-restricted (R) DFT (R-BLYP) solutions for the low-spin (LS) singlet state should suffer the triplet instability.

Because of this triplet instability, the bonding UHF MOs for the lowest spin (LS) ($S = 0$) state of **1** are given by the left−right split orbitals, which are described by mixing of the bonding and antibonding MOs in eq 1 as follows.

$$\psi^+(X) = \cos\theta\,\phi(X) + \sin\theta\,\phi^*(X) = \cos\omega\,a(X) + \sin\omega\,b(X) \qquad (3a)$$

$$\psi^-(X) = \cos\theta\,\phi(X) - \sin\theta\,\phi^*(X) = \cos\omega\,b(X) + \sin\omega\,a(X) \qquad (3b)$$

where θ and ω are the MO and VB orbital mixing parameters, and a(X) and b(X) are the localized natural orbitals (LNO) defined by $\theta = 45°$ as follows:[6]

$$a(X) = (1/2)\{\phi(X) + \phi^*(X)\} \cong dX_a \qquad (4a)$$

$$b(X) = (1/2)\{\phi(X) - \phi^*(X)\} \cong dX_b \qquad (4b)$$

The LNOs mainly localized on one site have generally small tails on the other site, satisfying the orthogonality condition, and they reduce to the corresponding AOs at the dissociation limit. The different orbitals for different spins (DODS) MOs (eq 3) for the up- and down-spins in the singlet state of **1** are more or less localized on the left and right chromium atoms, respectively, because of strong electron correlations. The DODS MOs are also obtained by the U-BLYP and U-B2LYP[13b] calculations, although θ and ω in eq 3 are different among the three computational procedures employed here. As shown previously,[6] the DODS MOs are reduced to the symmetry-adapted MOs given by eq 1 at the weak correlation limit (MO limit; $\theta = 0°$), whereas they become equivalent to the LNO by eq 4 at the VB limit ($\theta = 45°$).

Figure 1 illustrates the DODS MOs obtained for **1** at the interatomic distance $R = 2.0$ Å by the U-B2LYP method. The δ orbitals are mainly localized on the left (a) and right (b) Cr atoms, respectively. The π orbitals are considerably delocalized over both Cr atoms, but they are still symmetry-broken. The same situation is recognized even for the σ orbitals. The σ, π, and δ DODS MOs for **1** are found to be spin-polarized and more or less localized on an atomic site, in contradiction to the symmetry-adapted closed-shell MOs. In fact, they are rather close to the perfect-pairing (PP) GVB orbitals.[16] The orbital shapes are thus responsible for the direct exchange coupling between the Cr(II) ions. The calculated results for **1** are also compatible with the weak temperature-dependent paramagnetism for the $Cr_2(O_2CR)_4L_2$ compounds (L = MeOH, etc.).[5]

2.2. Occupation Numbers and Bond Orders for Dinuclear Metal−Metal Systems. Since the DODS MOs in Figure 1 are more or less spatially symmetry-broken because of the electron repulsion effects, the broken symmetry (BS) character for unstable metal−metal bonds is defined by the weight (D_i) of the doubly excited configuration for each bonding and antibonding pair i (=σ, π, and δ) in the CI formalism.[6]

$$y_i = 2D_i = 1 - 2T_i/(1 + T_i^2) \qquad (5)$$

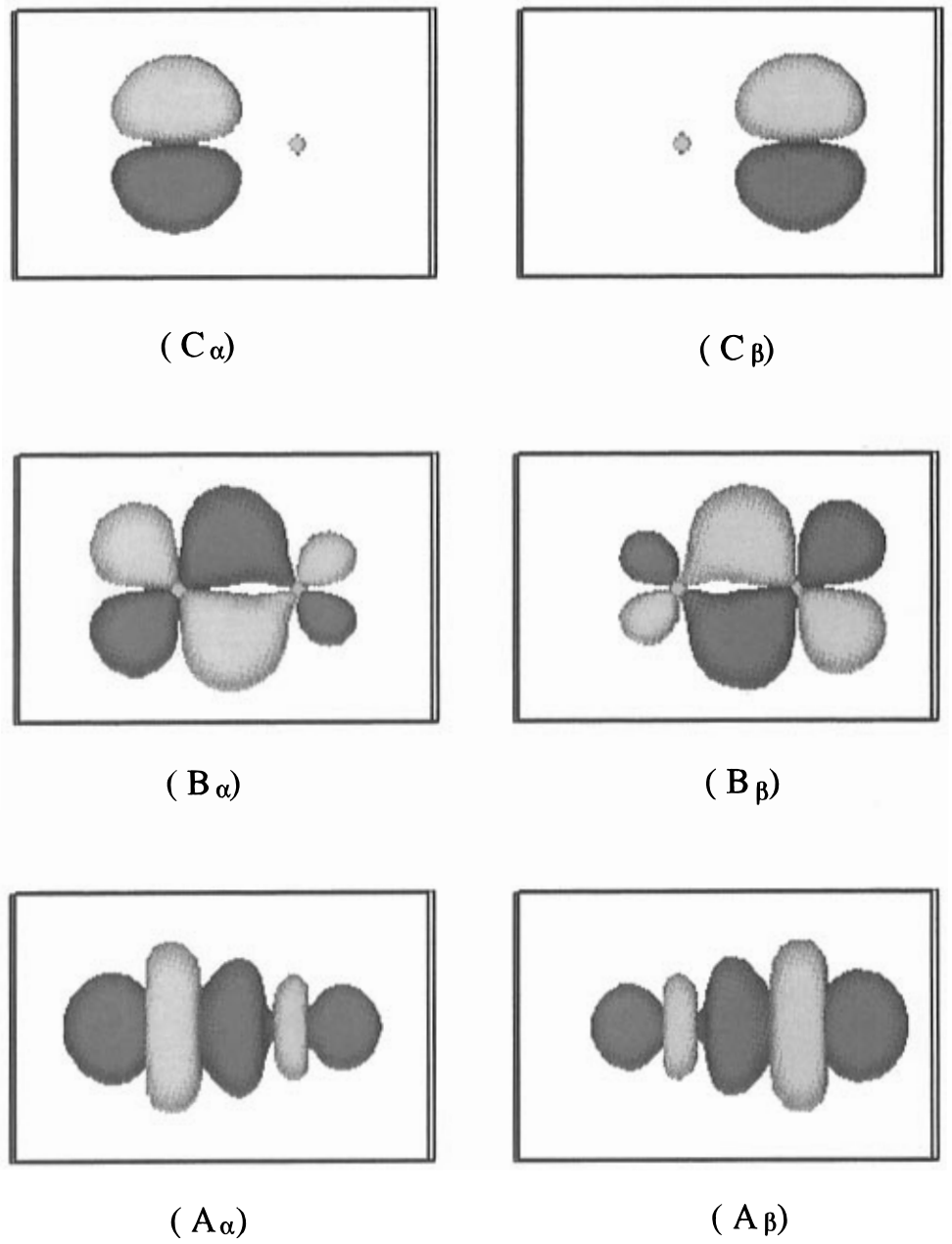

Figure 1. Computer graphics of the bonding DODS MOs for the naked Cr(II) dimer (**1**) obtained by the U-B2LYP method. A, B, and C denote the σ-, π-, and δ-type up (α) and down (β) spin orbitals.

It is also rewritten by the orbital overlap T_i between the split orbitals i under the UHF and DFT approximations, where the perfect-pairing (PP) approximation is employed for the spin projection.

$$T_i = \langle \psi_i^+ | \psi_i^- \rangle = \cos 2\theta \tag{6}$$

The BS character is the same as the diradical (DR) character (i.e., radical reactivity index) for organic DR species.[17] On the other hand, the BS character is somewhat related to the magnetic properties such as the weak paramagnetism[5] in the case of inorganic complexes or clusters.[8]

The natural orbitals (UNO) and their occupation numbers[6] of UHF and DFT solutions are determined by diagonalizing the first-order density matrices. The occupation numbers are expressed with the orbital overlap T_i as follows:

$$n_{\mathrm{HOMO}-i}(\mathrm{W}) = 1 + T_i \quad \text{and} \quad n_{\mathrm{LUMO}+i}(\mathrm{W}) = 1 - T_i \quad (i = 0, 1, 2) \tag{7}$$

where W = UHF or DFT. However, because of the spin contaminations, these occupation numbers are different from those of the spin-symmetry-adapted methods such as PP GVB, although the T_i value itself is usually close to the GVB value.[6] Then the occupation numbers in the PP-type spin-projected UHF or U-BLYP solutions are derived to obtain the spin-adapted values as[17,18]

$$n_{\mathrm{HOMO-i}}(\mathrm{PW}) = [n_{\mathrm{HOMO}-i}(\mathrm{W})]^2/(1 + T_i^2) = 2 - y_i \tag{8a}$$

$$n_{\mathrm{LUMO+i}}(\mathrm{PW}) = [n_{\mathrm{LUMO}+i}(\mathrm{W})]^2/(1 + T_i^2) = y_i \tag{8b}$$

where PW = PUHF or P-DFT. Therefore the effective bond order (BO) for a bond i is defined by

$$\mathrm{BO}_i = (n_{\mathrm{HOMO}-i}(\mathrm{PW}) - n_{\mathrm{LUMO}+i}(\mathrm{PW}))/2 = 2T_i/(1 + (T_i)^2) = 1 - y_i \tag{9}$$

From eqs 7−9, the effective bond order for the multiple metal−metal bond and occupation numbers are expressed by the BS character y_i.

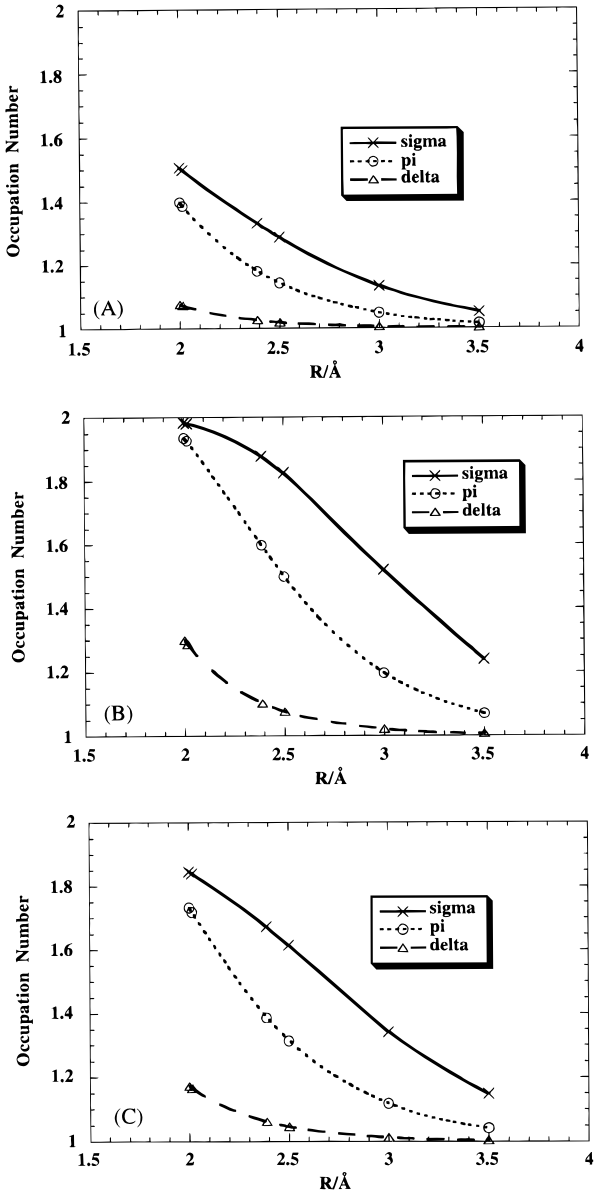

Figure 2. Variations of the occupation numbers for the σ-, π-, and δ-type natural orbitals (UNO) of the naked Cr(II) dimer (**1**) with the interatomic distance (R). A, B, and C show the calculated values by the spin-projected (P) UHF, U-BLYP, and U-B2LYP methods.

TABLE 2: Effective Bond Orders for the Naked Cr(II) Dimer (Cr_2^{4+}) by the PP-Type Projected UHF, U-BLYP, and U-B2LYP Methods

	PUHF			P-B2LYP			P-BLYP		
R/Å	σ	π	δ	σ	π	δ	σ	π	δ
2.000	0.506	0.398	0.076	0.846	0.733	0.172	0.983	0.935	0.300
2.015	0.499	0.386	0.072	0.840	0.719	0.165	0.981	0.926	0.287
2.389	0.332	0.180	0.025	0.673	0.386	0.061	0.878	0.598	0.101
2.500	0.287	0.143	0.019	0.614	0.314	0.046	0.826	0.499	0.076
3.000	0.133	0.048	0.005	0.341	0.118	0.013	0.519	0.196	0.021
3.500	0.052	0.015	0.001	0.148	0.042	0.003	0.239	0.069	0.006

The UHF, U-BLYP, and U-B2LYP calculations were carried out for **1**. Figure 2 shows variations of the occupation numbers calculated for the σ, π, and δ MOs (eq 1) by the spin-projected procedures (eq 8). Table 2 summarizes the effective bond orders calculated for **1** by eq 9.

From Table 2, and Figure 2, the following points are observed: (1) The occupation number of each bonding orbital for the d^4-d^4 exchange-coupled system **1** decreases monotonically with the increase of interatomic distance (R). (2) The occupation numbers calculated for the HOMO indicate the following tendency: n_{HO-i}(PU-BLYP) > n_{HO-i}(PU-B2LYP) > n_{HO-i}(PUHF). Probably, the PUHF provides the lower limit for the bond order, whereas the PU-BLYP gives the upper limit. (3) The occupation numbers of each bonding orbital for **1** by PU-B2LYP is smaller than the formal value, 2.0. Therefore, the corresponding bond order for each bond is also smaller than 1.0. Judging from the occupation number and bond order, the $\delta-\delta$ bond is particularly weak.[7] From these conclusions, the PP-type projection is useful for qualitative descriptions of the d−d bonding properties for the LS state. The bond order given by U-B2LYP is variable depending on the mixing ratio for the exchange potentials.[13b] We did not perform the reoptimization of the ratio for the metal−metal bonds. The sharp decrease of the σ and π bond orders in the range $2.3 < R < 2.5$ Å suggests that the nonlinear response properties for the external electromagnetic fields (second hyperpolarizability, hypermagnetiability, etc.) should exhibit characteristic variations because of electron fluctuation.[19]

TABLE 3: Effective Exchange Integrals (cm^{-1}) Calculated for the Naked Cr(II) Dimer (Cr_2^{4+}) by the Approximate Spin-Projected UHF, U-BYLP, and U-B2LYP Methods

R/Å	APUHF	APU-BLYP	APU-B2LYP
2.000	−565.5	−891.4	−1174.
2.015	−535.5	−850.2	−1118.
2.389	−136.0	−222.0	−332.0
2.500	−88.78	−140.4	−227.7
3.000	−12.00	−7.382	−34.50
3.500	−1.34	−0.006	−2.47

2.3. Effective Exchange Integrals. The UHF and DFT calculations clearly showed that the Cr(II)−Cr(II) bond is weak if the intermetallic distance exceeds 2.0 Å. The Heisenberg model is therefore utilized for their VB-like descriptions and for theoretical analysis of the weak paramagnetism.[5] The effective direct exchange integrals (J_{ab}) for **1** can be calculated by using an approximate spin projection (AP)[9d] procedure for the UHF and DFT solutions in combination with the Heisenberg model.[20−22]

$$J_{ab}(\text{APUHF or AP-DFT}) = [E(\text{LS}) - E(\text{HS})]/[\langle S^2\rangle(\text{HS}) - \langle S^2\rangle(\text{LS})] \quad (10)$$

where E(Y) and S^2(Y) denote, respectively, the total energy and total spin angular momentum for the spin state Y by UHF or DFT. It is noteworthy that the PP-type spin projection is inappropriate for calculations of J_{ab}[6,9e,16] since it neglects the spin-decoupling terms, which often play an essential role for subtle discussions of the HS−LS energy gaps[6] and the molecular magnetism.[3] Table 3 summarizes the J_{ab} values calculated for **1** by APUHF, APU-BLYP, and APU-B2LYP.

From Table 3 the following conclusions are drawn: (1) The effective exchange integrals calculated by all the methods are negative (antiferromagnetic), showing the weak covalent bond formation between the naked divalent chromium ions. (2) The magnitude of the J_{ab} values decreases with the increase of the Cr(II)−Cr(II) distance in an exponential manner. (3) The magnitude of the J_{ab} values shows the following tendency: $|J_{ab}$(APU-B2LYP)| > $|J_{ab}$(APU-BLYP)| > $|J_{ab}$(APUHF)|.

From conclusion 1, the antiferromagnetic exchange interaction between the Cr(II) ions can be described well in the approximate spin projection (AP) procedure,[20] in contradiction to the PP projection.[9e,16] Conclusion 3 is different from the tendency revealed from the calculated bond orders in section 2.2. This may be ascribed to the fact that the total energies of the HS and LS states by U-B2LYP involve the complex exchange terms.

TABLE 4: Effective Exchange Integrals J_{ab} (cm^{-1}) Calculated for the Naked Cr(II) Dimer (Cr_2^{4+}) by the Three Different Computational Procedures Based on the Total Energies by the UNO(UHF) CASCI and CASSCF Methods

	UNO CASCI			CASSCF		
R/Å	$J_{ab}(1)$	$J_{ab}(2)$	$J_{ab}(3)$	$J_{ab}(1)$	$J_{ab}(2)$	$J_{ab}(3)$
2.000	−805.9	−803.6	−810.5	−832.6	−824.1	−849.4
2.015	−752.3	−749.2	−758.3	−776.2	−767.4	−793.7
2.389	−156.2	−156.0	−156.7	−158.2	−157.1	−160.3
2.500	−100.5	−100.5	−100.5	−101.5	−101.0	−102.5
3.000	−13.00	−13.01	−12.99	−13.07	−13.02	−13.18

3. CASCI and CASSCF Calculations by the Use of UNO

The spin-unrestricted approaches such as UHF and U-BLYP often suffer the so-called spin contamination errors. The PP and AP spin projection procedures described above are utilized to remove them, particularly in the low-spin (LS) state. It is clear that the more refined MCSCF method is desirable for quantitative purpose. However, the GVB PP method, which is regarded as a simplied MCSCF, is not so effective for computations of the magnetic interactions because of lack of spin-decoupling (polarization) terms. So, the complete active space (CAS) CI and CASSCF treatments involving them are inevitable for the purpose. Judging from the occupation numbers in eq 7, the eight active orbitals and eight electrons {8, 8} are at least necessary for the CASCI and CASSCF[23−25] calculations of **1** in order to confirm the APUHF and AP-DFT results. Here, UNOs determined by UHF and U-B2LYP were utilized for UNO CASCI and as the trial orbitals for CASSCF calculations.[6] The CASSCF convergence was very good for the U-B2LYP trial. Since the U-B2LYP SCF calculation itself exhibits a rapid convergence, the present procedure will be useful for the CASSCF calculations of complex transition-metal systems. The UNO CASCI and CASSCF calculations were carried out using the HONDO 95 program package.[26]

To examine the reliability of the spin multiplet splittings by the Heisenberg model, the J_{ab} values for the direct exchange coupling between the Cr(II) ions were calculated from total energies $E(Z)$ by UNO CASCI and CASSCF methods[6] as follows:

$$J_{ab}(1) = (E(\mathrm{S}) - E(\mathrm{Q}))/6 \qquad (11a)$$

$$J_{ab}(2) = (E(\mathrm{T}) - E(\mathrm{Q}))/4 \qquad (11b)$$

$$J_{ab}(3) = (E(\mathrm{S}) - E(\mathrm{T}))/2 \qquad (11c)$$

where S, T, and Q (=*Z*) denote, respectively, the singlet, triplet, and quintet states. Therefore, if these J_{ab} values are nearly equal, $J_{ab} \cong J_{ab}(1) \cong J_{ab}(2) \cong J_{ab}(3)$, the energy splittings are reduced to those of the Heisenberg model. Table 4 summarizes the $J_{ab}(1)$, $J_{ab}(2)$, and $J_{ab}(3)$ values obtained for **1** by UNO CAS CI and CASSCF {8, 8} methods.

From Table 4, conclusions are as follows: (1) The J_{ab} values by UNO(UHF) CASCI and CASSCF are almost equivalent, and these are rather close to the U-BYLP values. (2) For **1**, the $J_{ab}(1)$, $J_{ab}(2)$, and $J_{ab}(3)$ values are almost equal to one another. This is in good agreement with the energy splittings expected from the Heisenberg model.

From conclusion 1, U-BLYP can be utilized for computations of J_{ab} for larger systems instead of UNO CASCI and CASSCF. Judging from previous results,[20] the J_{ab} values by CASPT2 could be reproduced by U-B2LYP. Since the CASSCF and CASPT2 calculations are time-consuming for larger transition-metal clusters, the DFT-based procedures would be useful for the practical calculations of transition-metal clusters.

4. Naked Tetranuclear Cr(II) Systems

4.1. UHF and DFT Calculation. The d−d conjugated systems are interesting targets from several theoretical viewpoints: magnetism, optical nonlinearity, magnetooptics, and so on.[3,6,8,19] Here, the linear naked tetramer {$Cr(II)_a$−$Cr(II)_b$−$Cr(II)_c$−$Cr(II)_d$} (**6**) of the Cr(II) ion with the equivalent interatomic distance was investigated as an example using the TZ basis set[12] by the UHF and U-B2LYP methods. The first-order density matrices obtained by these methods were diagonalized to obtain the natural orbitals and their occupation numbers for **6**. Judging from the occupation numbers, four valence orbitals should be active for each symmetry. Therefore 16 active orbitals and 16 active electrons are regarded as CAS {16, 16} for **6**.

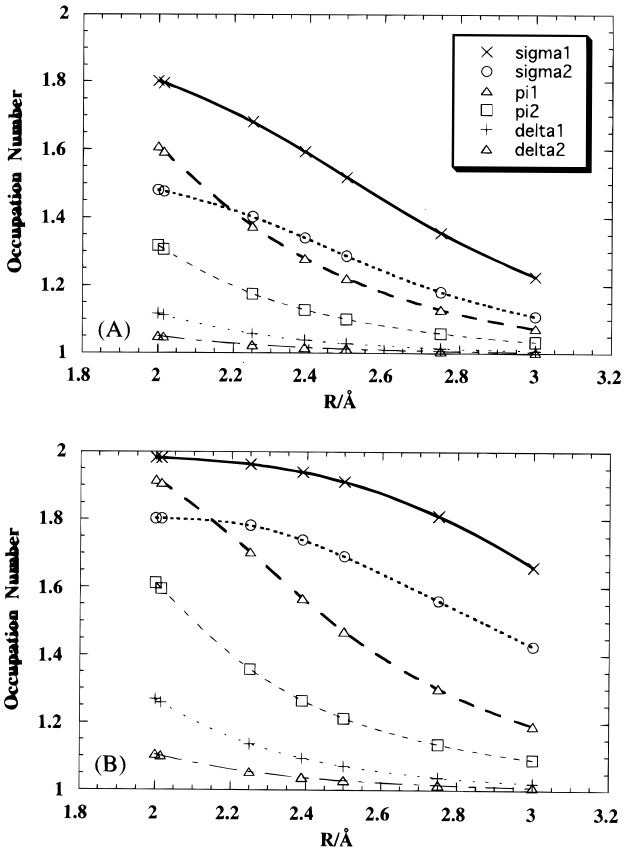

Figure 3. Variations of the occupation numbers for the σ-, π-, and δ-type natural orbitals (UNO) of the naked Cr(II) tetramer (**6**) with the interatomic distance (R). A and B show the calculated values by the spin-projected (P) UHF and U-B2LYP methods.

Since the UNO CASCI and CASSCF {16, 16} calculations would be impossible at the present time, the spin-projected UHF and DFT calculations were carried out for a qualitative purpose. The four bonding DODS MOs for each symmetry are given by the mixing of the UNOs as

$$\psi^{\pm}{}_1(X) = \cos\theta_1\,\phi_1(X) \pm \sin\theta_1\,\phi_4(X) \qquad (12a)$$

$$\psi^{\pm}{}_2(X) = \cos\theta_2\,\phi_2(X) \pm \sin\theta_2\,\phi_3(X) \qquad (12b)$$

where θ_i is the orbital mixing parameter for UNOs: $\phi_i(X)$, i = 2(3) for HOMO(LUMO) and i = 1(4) for the next HOMO-(LUMO) with each symmetry. The UNOs are given by

$$\phi_i(X) = N[c_a\mathrm{d}X_a + c_b\mathrm{d}X_b + c_c\mathrm{d}X_c + c_d\mathrm{d}X_d]\ (i = 1{-}4) \qquad (13)$$

where c_f is the LCAO coefficient at the site f (=a, b, c, d) and N is the normalizing factor. The occupation numbers for two π-bonding natural orbitals in eq 13 are given by eqs 6, 7, 8, and 11 from PUHF and P-DFT calculations. Figure 3 illustrates variations of the occupation numbers with the change of the

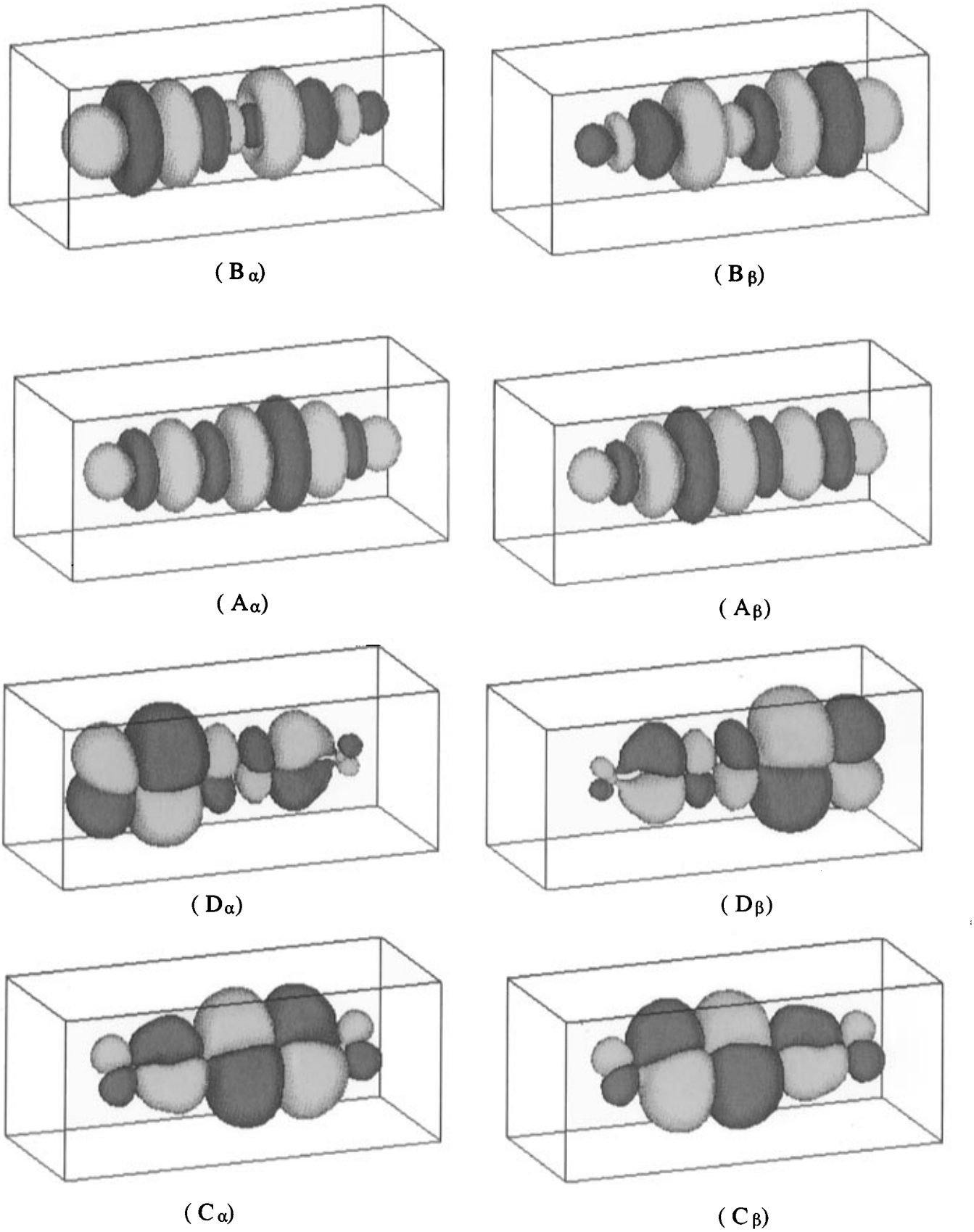

Figure 4. Computer graphics of the two bonding DODS MOs for the naked Cr(II) tetramer (**6**) obtained by the U-B2LYP method. A and B denote the σ-type next HOMO and the HOMO for the up (α) and down (β) spins. Similarly, C and D denote the corresponding π-type orbitals.

interatomic distance (R) for **6**. Figure 4 illustrates the four DODS bonding MOs (eq 11) with σ or π symmetry.

From Figures 3 and 4, the following points are observed: (1) The occupation number for the next HOMO with each symmetry is much larger than the corresponding value for the HOMO. This is ascribed to the d−d conjugation effect. (2) The occupation numbers for the σ HOMO ($i = 0$ in eq 8) and the next σ HOMO ($i = 1$ in eq 8) for **6** are larger than 1.5 even at $R = 2.5$ Å under the B2LYP approximation. The d−d conjugation effect is strong for the σ orbitals. In fact, the σ DODS MOs are almost paired at $R = 2.0$ Å. (3) The occupation number for the π HOMO of **6** is smaller than the corresponding

TABLE 5: Spin Densities Calculated for the Naked Cr(II) Dimer (Cr_2^{4+}) by the UHF, U-BLYP, and U-B2LYP Methods

R/Å	UHF a(−b)	U-BLYP a(−b)	U-B2LYP a(−b)
2.0	3.860	2.954	3.559
2.015	3.863	2.999	3.574
2.389	3.904	3.598	3.759
2.500	3.916	3.677	3.792
3.00	3.970	3.887	3.917
3.50	3.988	3.965	3.970

TABLE 6: Spin Densities Calculated for the Naked Cr(II) Tetramer (Cr_4^{8+}) by the UHF and U-B2LYP Methods

	UHF		U-B2LYP	
R/Å	a(−d)	b(−c)	a(−d)	b(−c)
2.0	3.611	−4.263	3.248	−3.802
2.015	3.621	−4.256	3.262	−3.824
2.25	3.804	−3.792	3.519	−3.517
2.389	3.908	−3.581	3.693	−3.155
2.50	3.961	−3.577	3.803	−3.037
2.75	3.997	−3.778	3.912	−3.244
3.00	3.995	−3.911	3.934	−3.572

value for **1**. The π DODS MOs are therefore significantly spin-polarized and are more or less localized on the left and right Cr(II) dimer group regions of **6** even at $R = 2.0$ Å.

Conclusions 1 and 2 for **6** are consistent with the metallic character, while conclusion 3 is compatible with the spin density wave (SDW) character for the chromium metal. The sharp variations of the π bond orders in the region $2.2 < R < 2.5$ Å suggest that several electronic properties such as the hyperpolarizability and hypermagnetability are controllable by changing the interatomic distances for the tetranuclear Cr(II) complexes with ligands and other structural factors.[8] Therefore experimental studies on the d−d conjugated systems are very interesting from this point of view.

4.2. Spin Densities. The SDW-type spin density alternation disappears because of the very fast quantum spin fluctuation (or resonance) in the case of small clusters such as **6**. In fact, the spin projection procedure is responsible for the isotropic rotation of the spin vector, retaining the antiferromagnetic spin correlation ($\uparrow\downarrow$) described by the scalar product of the spin vector $\mathbf{S_a}\cdot\mathbf{S_b} < 0$.[27] Tables 5 and 6 summarize, respectively, the total atomic spin densities (Q_f) obtained for **1** and **6** by UHF, U-BLYP, and U-B2LYP. From Table 5, the magnitude of the calculated spin densities for **1** is quite similar between UHF and U-B2LYP. On the other hand, the spin densities on site c for **6** at $R = 2.0$ Å are about 4.3 and 3.8, respectively, by UHF and U-B2LYP. The UHF calculation clearly overestimates the spin polarization on the inner Cr(II) atoms for **6**. The U-BLYP values would be too small because of the lack of the self-interaction correction (SIC).[28] It is well-known that the DFT without SIC underestimates the stability of the antiferromagnetic state for copper oxides and other transition metal complexes.[9d] The magnitude of the spin density becomes close to the classical value 4.0 for both **2** and **6** at a long interatomic distance.

5. Discussion

5.1. Direct Exchange Couplings. According to Benard's ab initio instability analysis,[29] the triplet instability occurs even in the case of the Cr(II)$(O_2CH)_4$ dimer. This implies that the orbital mixings (eq 3) between the bonding and antibonding MOs in eq 1 are not zero for its quadruple bond; namely, the contribution of the multiple excitations to the ground configuration is significant even if the $(O_2CH)_4$ ligands are added to the naked core **1**. This in turn indicates that the effective exchange integrals calculated for the naked core **1** would be useful for qualitative discussion of magnetism observed for the binuclear complexes.[5]

The $Cr_2(O_2CR)_4L_2$ compounds (L = MeOH, etc.)[5] (**7**) and their solvates have consistently been found to show weak paramagnetism, usually corresponding to about 0.3−0.5 μ_B at room temperature. The absolute J_{ab} values for these species should be over 500 cm^{-1}. The J_{ab} values in Tables 3 and 4 were fitted with the single-exponential function

$$J_{ab} = -p \exp(-qR) \tag{14}$$

where p and q are the fitting parameters. The direct effective exchange integrals for the core **1** in several binuclear complexes were estimated using the J_{ab} fitting curves, assuming their observed Cr−Cr distances.[5,6] The estimated results by CASSCF and U-B2LYP are summarized in Table 7.

TABLE 7: Effective Exchange Integrals (J_{ab}) Estimated for Several Binuclear Cr(II) Complexes (7a−7l) by the CASSCF and U-B2LYP Methods, Together with the Experimental Values[a]

no.	compound	*R*/Å	J_{ab}(CASSCF)[b]	J_{ab}(U-B2LYP)[c]	exptl[d]
7a	$Cr_2(DMP)_4$	1.847	−1474	−1831	
7b	$Cr_2[PhNC(CH_3)O]_4$	1.873	−1334	−1694	
7c	$Cr_2(mhp)_4$	1.889	−1255	−1614	
7d	$Cr_2(CO_3)_4(H_2)_2$	2.214	−361.7	−668.6	
7e	$Cr_2(O_2CMe)_4(MeOH)_2$	2.329	−232.9	−431.0	−502
7f	$Cr_2(O_2CMe)_4(H_2O)_2$	2.362	−205.3	−390.3	−490
7g	$Cr_2(O_2CMe)_4(py)_2$	2.369	−199.9	−382.2	−479
7h	$Cr_2(O_2CH)_4(2H_2O)_2$	2.373	−196.8	−377.6	
7i	$Cr_2(O_2CNEt_2)_4(NHEt_2)_2$	2.384	−188.7	−365.4	−298
7j	$Cr_2(O_2CMe)_4(MeCN)_2$	2.396	−180.3	−352.5	−463
7k	$Cr_2(O_2CH)_4(PY)_2$	2.408	−172.2	−334.0	
7l	$Cr_2(O_2CCF_3)_4(Et_2O)_2$	2.541	−103.5	−228.1	−231

[a] The estimation was carried out using the J_{ab} values calculated for the naked Cr(II) dimer (Cr_2^{4+}) (see text). [b] $p = 1.731 \times 10^6$, $q = 3.827$. [c] $p = 4.682 \times 10^5$, $q = 3.002$ in eq 13. [d] Reference 5.

The absolute J_{ab} values estimated by both methods become over 1000 cm^{-1} for **1** in the complexes with short Cr−Cr bonds ($R < 1.95$ Å), which are diamagnetic, in conformity with experiments.[5] The magnitude of the J_{ab} value by CASSCF is about 50% of the corresponding experimental value. Similarly, the DFT(U-B2LYP) absolute value is uniformly smaller than the experimental one except for **7i**. The calculated J_{ab} value by U-B2LYP is −228 cm^{-1} for $Cr_2(O_2CCF_3)_4(Et_2O)$ (**7l**), which has the largest Cr−Cr distance among the complexes cited in Table 7. This value is compatible with the experiment.[5] However, the calculated values do not involve the through-bond exchange coupling between the $d_{x^2-y^2}$ orbital of Cr and the exchange coupling via the σ system of the acetate anion ligand in the complex. Therefore, the difference between the calculated and experimental J_{ab} values should be ascribed to these ligand effects. Theoretical studies on the ligand effects are apparently necessary even for qualitative purposes.

5.2. Quantum Tunneling in Large Magnetic Clusters. The ab initio UHF and DFT calculations are in principle feasible for large clusters of Cr(II) and other transition-metal ions (M = Cr^{3+}, Mn^{2+}, Fe^{3+}, etc) to elucidate their electronic structures. Since such first-principle calculations are time-consuming, several model Hamiltonians are derived for each purpose. For example, judging from the magnitude of the spin density in Tables 5 and 6, the Heisenberg spin Hamiltonian[6,30] can be used for investigation of the magnetism for Cr(II) clusters,

$$H = -2\sum J_{ab}\mathbf{S_a}\cdot\mathbf{S_b} \tag{15}$$

where $\mathbf{S_c}$ denotes the spin at the site c, and J_{ab} is given by the ab initio calculations.[9] If J_{ab} is negative in sign for the direct exchange and superexchange coupled transition-metal ions, large

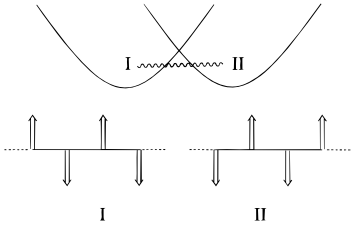

Figure 5. Schematic illustration of the quantum spin tunneling for the mesoscopic antiferromagnetic complexes. I and II denote, respectively, the antiferromagnetic spin alignments.

linear or cyclic clusters in Figure 5 should exhibit the antiferromagnetic spin alignments.[9]

Recently large magnetic clusters have received interest in relation to several interesting phenomena: magnetic bistability, spin crossover induced by the external magnetic field, spin tunneling, so on.[6,11,19] The spin inversions for mesoscopic clusters having short-range antiferromagnetic orders have been discussed in relation to the macroscopic quantum tunneling in the field of solid state physics.[11,31] Probably, magnetic dots, wires, and rings with finite cluster sizes will be synthesized using the transition-metal ions with and without ligands by several physical and chemical techniques.[19,32] The electronic properties of such large d−d conjugated systems will become interesting targets for the quantum dynamics based on the model Hamiltonians derived from the ab initio UHF and DFT calculations.

5.3. Concluding Remarks. The computational procedures UHF,[17] DFT,[7] their approximate spin-projected versions (AP-UHF, AP-DFT),[9] CASCI[23] by the use of the UHF natural orbitals (UNO), and UNO CASSCF[24,25] were successfully applied to ab initio calculations of the effective bond orders and effective exchange integrals for the naked Cr(II) dimer and tetramers. These species were found to be particularly appropriate for detailed explanation of the above theoretical and computational methods because of strong electron correlation. The present approaches have no methodological limitation even for binuclear, tetranuclear, and larger multicenter complexes with ligands. The computations for bi- and tetranuclear systems with ligands are now in progress to elucidate the through-ligand interactions between the Cr(II) ions. The Heisenberg Hamiltonian involving the ab initio J_{ab} values is often useful for investigation of spin properties of such large systems.[3,6] In fact, its application to molecular magnetism has been performed in other papers.[33]

Acknowledgment. One of the authors (K.Y.) would like to thank Professor S. Nagakura for his continuous encouragement for theoretical studies on molecular magnetism and molecular spinics. The authors thanks Professors A. Nakamura, K. Tani, W. Mori, and K. Mashima for helpful discussions and comments. They also gratefully acknowledge the financial support of the Ministry of Education, Science and Culture of Japan (Specially Promoted Research No. 06101004).

References and Notes

(1) Cotton, F. A.; Walton, R. A. *Multiple Bonds between Metal Atoms*; Clarrendon Press: Oxford, 1993, and references therein.

(2) (a) Slater, J. C. *Adv. Quantum Chem.* **1972**, *6*, 1. (b) Tiegler, T. *J. Am. Chem. Soc.* **1984**, *106*, 5901.

(3) Gatteschi, D., Kahn, O., Miller, J. S., Palacio, F., Eds. *Magnetic Molecular Materials*; NATO ASI Series 198; Kluwer Academic Publishers: London, 1991.

(4) (a) Cotton, F. A. *Acc. Chem. Res.* **1978**, *11*, 225. (b) Chisholm, M. H.; Cotton, F. A. *Acc. Chem. Res.* **1978**, *11*, 356.

(5) (a) Cotton, F. A.; Eglin, J. L.; Hong, B.; James, C. A. *J. Am. Chem. Soc.* **1992**, *114*, 4915. (b) Cotton, F. A.; Chen, L.; Daniels, L. M.; Feng, X. *J. Am. Chem. Soc.* **1992**, *114*, 8980.

(6) Yamaguchi, K. *Self-Consistent Field: Theory and Applications*; Carbo, R., Klobukowski, M., Eds.; Elsevier: Amsterdam, 1990; p 727.

(7) (a) Yamaguchi, K. *Chem. Phys. Lett.* **1979**, *66*, 395. (b) *Ibid.* **1979**, *68*, 477.

(8) (a) Nishino, M.; Tanaka, M.; Takeda, S.; Mashima, K.; Wori, W.; Tani, K.; Nakamura, A.; Yamaguchi, K. *Mol. Cryst. Liq. Cryst.*, in press. (b) *Ibid.*, in press.

(9) (a) Yamaguchi, K.; Tsunekawa, T.; Toyoda, Y.; Fueno, T. *Chem. Phys. Lett.* **1988**, *143*, 371. (b) Takahara, Y.; Yamaguchi, K.; Fueno, T. *Chem. Phys. Lett.* **1989**, *158*, 95. (c) Yamaguchi, K.; Fueno, T.; Ueyama, K.; Nakamura, A.; Ozaki, M.-A. *Chem. Phys. Lett.* **1990**, *168*, 56. (d) Yamaguchi, K.; Takahara, Y.; Fueno, T. In *Applied Quantum Chemistry*; Smith, V. H., Jr., Schaefer, H. F., III, Morokuma, K., Eds.; Reidel: Dordrecht, 1986; p 155. (e) Yamanaka, S.; Kawakami, T.; Noro, T.; Yamaguchi, K. *J. Mol. Struct. (THEOCHEM)* **1994**, *310*, 185.

(10) Baumann, C. A. van Zee, R. J.; Bhat, S. B.; Welter, Jr. *J. Chem. Phys.* **1983**, *78*, 190.

(11) (a) Awschalom, D. D.; DiVincenzo, D. P.; Smyth, J. F. *Science* **1992**, *258*, 414. (b) Awschalon, D. D.; Smyth, J. F.; Grinstein, G.; DiVincengo, D. P.; Loss, D. *Phys. Rev. Lett.* **1992**, *68*, 3092.

(12) Tatewaki, H.; Hujinaga, S. *J. Chem. Phys.* **1980**, *72*, 4339.

(13) (a) Becke, A. D. *Phys. Rev. A* **1988**, *38*, 3098. (b) Becke, A. D. *J. Chem. Phys.* **1993**, *98*, 1372. (c) Edgecombe, K. E.; Becke, A. D. *Chem. Phys. Lett.* **1995**, *244*, 427.

(14) Lee, C.; Yamg, W.; Parr, R. G. *Phys. Rev. B* **1988**, *37*, 785.

(15) Frisch, M. J.; Trucks, G. W.; Schlegel, H. B.; Gill, P. M. W.; Johnson, B. G.; Robb, M. A.; Cheeseman, J. R.; Keith, T. A.; Petersson, G. A.; Montgomery, J. A.; Raghavachari, K.; Al-Laham, M. A.; Zakrzewski, V. G.; Oritiz, J. V.; Foresman, J. B.; Cioslowski, J.; Stefanov, B. B.; Nanayakkara, A.; Challacombe, M.; Peng, C. Y.; Ayala, P. Y.; Chen, W.; Wong, M. W.; Andres, J. L.; Replogle, E. S.; Gomperts, R.; Martin, R. L.; Fox, D. J.; Binkley, J. S.; Defrees, D. J.; Baker, J.; Stewart, J. P.; Head-Gordon, M.; Gonzalez, C.; Pople, J. A. *GAUSSIAN 94*; Gaussian, Inc.: Pittsburgh, PA, 1995.

(16) (a) Googgame, M. M.; Goddard, W. A., III. *Phys. Rev. Lett.* **1982**, *48*, 135. (b) Googgame, M. M.; Goddard, W. A., III. *J. Phys. Chem.* **1981**, *85*, 215.

(17) Yamaguchi, K. *Chem. Phys. Lett.* **1975**, *33*, 330.

(18) Takatsuka, K.; Fueno, T.; Yamaguchi, K. *Theor. Chim. Acta* **1978**, *48*, 176.

(19) Yamaguchi, K.; Gatteschi, D. NATO ASI Series, in press.

(20) Yamanaka, S.; Kawakami, T.; Nagao, H.; Yamaguchi, K. *Chem. Phys. Lett.* **1994**, *231*, 25.

(21) Our approximate spin projection scheme described in this article was independently presented in refs 6, 7, 9d, 18, and 19 from the Needleman-Davidson scheme for the spin-unrestricted DFT solution (ref 22).

(22) (a) Noodleman, L. *J. Chem. Phys.* **1981**, *74*, 5737. (b) Noodleman, L.; Davidson, E. R. *Chem. Phys.* **1987**, *109*, 131.

(23) The CASCI, CASSCF, and CAS coupled-cluster (CC) starting from UNO were presented in ref 24. See also the papers (ref 25) by Pulay and his co-workers.

(24) Yamaguchi, K. *Int. J. Quantum Chem.* **1980**, *S14*, 267.

(25) (a) Pulay, P.; Hamilton, T. P. *J. Chem. Phys.* **1988**, *88*, 4926. (b) Bofill, J. M.; Pulay, P. *J. Chem. Phys.* **1989**, *90*, 3657.

(26) Dupuis, M.; Marquez, A.; Davidson, E. R. *HONDO 95.3 from CHEM-Station*; IBM Corp.: Neighborhood Road, Kingston, NY 12401, 1995.

(27) The spin correlation functions for finite systems were discussed thoroughly: (a) Yamaguchi, K.; Fueno, T. *Chem. Phys.* **1977**, *19*, 35. (b) Yamaguchi, K. *Chem. Phys.* **1978**, *29*, 117.

(28) Yamanaka, S.; Kawakami, T.; Yamada, S.; Nagao, H.; Nakano, M.; Yamaguchi, K. *Chem. Phys. Lett.* **1995**, *240*, 268.

(29) Benard, M. *J. Chem. Phys.* **1979**, *71*, 2546. (b) Benard, M. *J. Am. Chem. Soc.* **1978**, *100*, 2354.

(30) Yamaguchi, K.; Yoshioka, Y.; Fueno, T. *Chem. Phys.* **1977**, *20*, 171.

(31) (a) Chudnovsky, E. M.; Gunter, L. *Phys. Rev. Lett.* **1988**, *60*, 661. (b) Awshalorm, D. D.; Smyth, J. F.; Grinstein, G.; DiVincenzo, D. P.; Loss, D. *Phys. Rev. Lett.* **1992**, *68*, 3092. (c) Awaga, K.; Tatara, G.; Fukuyama, H. *J. Phys. Soc. Jpn.* **1993**, *62*, 1939. (d) Tatara, G.; Fukuyama, H. *Phys. Rev. Lett.* **1994**, *72*, 772.

(32) Gatteschi, D.; Caneschi, A.; Pardi, L.; Sessoli, R. *Science* **1994**, *265*, 1054.

(33) (a) Okumura, M.; Yamaguchi, K.; Nakano, M.; Mori, W. *Chem. Phys. Lett.* **1993**, *207*, 1. (b) Okumura, M.; Mori, W.; Yamaguchi, K. *Chem. Phys. Lett.* **1994**, *219*, 36.